Modeling of Schottky barrier modulation due to oxidation

at metallic electrode and semiconducting carbon nanotube junction

Toshishige Yamada[a]

NASA Ames Research Center, M/S 229-1, Moffett Field, California, 94035-1000

A model is proposed for the previously reported lower Schottky barrier for holes Φ_{Bh} in air than in vacuum at a metallic electrode − semiconducting carbon nanotube (CNT) junction. We assume that there is a transition region between the electrode and the CNT, and an appreciable potential can drop there. The role of the oxidation is to increase this potential drop with negatively charged oxygen molecules on the CNT, leading to lower Φ_{Bh} after oxidation. The mechanism prevails in both p- and n-CNTs, and the model consistently explains the key experimental findings.

In air, a carbon nanotube (CNT) is oxidized and oxygen molecules stay at the CNT surface. The IBM group built CNT field-effect transistors (FETs) [1] and measured the channel conductance g_d as a function of gate voltage V_G. They concluded that the Schottky barrier Φ_B between the metallic electrode and the semiconducting CNT at the source or drain contact was modulated in oxidation [2]. In vacuum, g_d rose slowly at $V_{G1} < 0$ and rapidly at $V_{G2} > 0$ in Fig. 1(a) because Φ_B for holes (Φ_{Bh}) was high and Φ_B for electrons (Φ_{Be}) was low as in the band structures at V_{G1} and V_{G2} in Figs. 1(b) and 1(c), respectively, where the CNT conduction and valence edges are shown and α is a device constant [3]. In air, the g_d asymmetry flipped in Fig. 1(d) because Φ_{Bh} was low and Φ_{Be} was high due to oxidation as in the band structures at V_{G3} and V_{G4} in Figs. 1(e) and 1(f), respectively. If the main role of oxidation had been to dope the bulk CNT p-type rather than to modify Φ_B, the entire g_d-V_G characteristics would have simply shifted horizontally without the g_d asymmetry flip. This is the basis of the Φ_B modulation in oxidation.

In this letter, we propose a model and explain how Φ_{Bh} can *decrease* in oxidation. The oxidation seems to result in the opposite, i.e., an *increase* in Φ_{Bh} at first glance. In fact, oxygen molecules are expected to be negatively charged on the CNT because of the large electronegativity. The negative charge may not necessarily come only from the CNT, but also from the environment [4]. Generally, negative charge at the material surface will *increase* the surface dipole providing the confinement mechanism for electrons within the material bulk [4]. Thus, the CNT electron affinity ϕ_s should *increase* in oxidation such that $\phi_s < \phi_s'$, where a quantity in vacuum is denoted without a prime and that in air is denoted with a prime. According to the standard band-alignment theory at the interface [5], Φ_{Bh} is determined with the electron work function χ_m of the metallic electrode and ϕ_s by $\Phi_{Bh} = E_G + \phi_s - \chi_m$ as in Fig. 2(a), where the CNT conduction and valence edges are shown with the band gap E_G and the Fermi energy ζ. The influence of oxidation appears

only in ϕ_s, and we will have $\Phi_{Bh} < \Phi_{Bh}'$ and $\Phi_{Be} = E_G - \Phi_{Bh} > \Phi_{Be}' = E_G - \Phi_{Bh}'$ in Fig. 2(b) after oxidation, but these relations are contradictory to the experimental results [2].

This view is defective in two ways. (1) It assumes that the metallic electrode – semiconducting CNT junction is so abrupt that there is no transition region between the electrode and the CNT and there is no appreciable potential drop there. However, this may not be the case. (2) Indeed ϕ_s will increase in oxidation and become ϕ_s' ($> \phi_s$) on a *free* CNT surface [6]. However, in the *junction structure* consisting of the electrode and the CNT, it is not certain whether the oxidation effect can be represented as the electronic property modulation in the CNT side only [7]. A cruder way to say this is that the work functions of the electrode and the CNT should be both modified in oxidation, but from the beginning, the separate work functions will not have meaning in the junction structure.

Our model overcomes these difficulties. We assume a transition region between the electrode and the CNT, where an appreciable potential ΔU can drop. We will argue that ΔU is modified in oxidation, and this explains the Φ_B difference in vacuum and in air [2], by taking an example of a p-CNT for illustration, but the same mechanism will also work for an n-CNT. In vacuum in Fig. 2(c), ΔU is small. The p-CNT depletes near the junction interface, and the depletion region provides negative charge. This negative charge is neutralized by the positive charge on the CNT and the other positive charge on the electrode. In air in Fig. 2(d), $\Delta U'$ is large, since the oxygen is negatively charged at the CNT surface and raises the potential at the interface. This negative charge is neutralized by the positive charge in the CNT and the other positive charge on the electrode. In this picture, we have $\Phi_{Bh} = \phi_s + E_G - \chi_m - \Delta U$. The effect of oxidation appears only in ΔU, and ΔU in vacuum is smaller than $\Delta U'$ in air. Therefore, $\Phi_{Bh} > \Phi_{Bh}'$ and accordingly $\Phi_{Be} < \Phi_{Be}'$, which are the correct relations consistent with the experiments [2].

The role of V_G in a CNT FET is to change the channel doping effectively. With the application of V_G, positive and negative charges are introduced as in Fig. 3(a). The electric field is mostly vertical, and the horizontal component is negligible due to the extremely thin geometry of the CNT. If we consider a band structure along the arrow path from the metallic source, through the CNT, to the metallic drain, the band bending occurs only in the depletion regions below the source and the drain since the path is parallel to the electric field only there. Thus, the energy band structure with the CNT conduction and valence edges will have a shape in Fig. 3(b), where A-D indicate corresponding points on the path. The negative charge density in the depletion region in the band picture has to be consistent with the induced carrier density in the CNT channel. Thus, the effect of V_G can be absorbed in the redefinition of ζ and the effective background doping density N_B. The charge neutrality relation holds for both the original and the equivalent band pictures.

We will derive a relation for the CNT band bending ϕ_0 and ΔU based on this charge neutrality relation, assuming that the oxygen molecules are negatively charged and phyisorbed to the CNT, so that their charge σ_{ox} is constant, independent of ϕ_0 and ζ. There are charge σ_m on the metallic electrode and charge σ_{NT} within the CNT in the depletion or accumulation mode. The neutrality relation requires $\sigma_m + \sigma_{ox} + \sigma_{NT} = 0$, and this determines ΔU as a function of ϕ_0. Before discussing analytical solutions, we will find solutions graphically through the intersection of two graphs $\sigma = -\sigma_m(\phi_0) = [\chi_m - (\phi_s + \phi_0 + \zeta)]\varepsilon_{tr}/ea$ and $\sigma = \sigma_{NT}(\phi_0) + \sigma_{ox}$, where ε_{tr} is a dielectric constant, a is a width of the transition region, and e is the unit charge. The intersection defines ϕ_0 and $\Delta U = e\sigma_m(\phi_0)/C_G$. Then, we calculate $\Phi_{Bh} = \phi_s + E_G - \chi_m - \Delta U$ and $\Phi_{Be} = \chi_m + \Delta U - \phi_s$.

$\sigma = -\sigma_m(\phi_0)$ is a straight line like "ka" with a negative slope. It depends on the CNT only through ζ, and its functional form is the same for p- and n-CNTs. $\sigma = \sigma_{NT}(\phi_0) + \sigma_{ox}$ is different for p- and n-CNTs as in Figs 4(a) and 4(b), and we will examine these scenarios separately. In the

p-CNT scenario, accumulation occurs for $\phi_0 > 0$ and positive $\sigma_{NT}(\phi_0)$ increases rapidly with ϕ_0, while inversion occurs for $\phi_0 < 0$ and negative $\sigma_{NT}(\phi_0) = -(2\varepsilon_{NT}\phi_0 N_B)^{1/2}$ is a horizontal parabola with the planar junction theory [5]. In vacuum, $\sigma_{ox} = 0$ and $\sigma_{NT}(\phi_0)$ is line "$\alpha 0$" in Fig. 4(a). As the oxidation progresses and σ_{ox} becomes more negative, $\sigma_{NT}(\phi_0) + \sigma_{ox}$ shifts downward and forms lines "$\alpha 1$" and "$\alpha 2$". Thus, the intersection moves down from A0 through A1 to A2. This means that the band bending is large downward $\phi_{0A0} < 0$ in vacuum at A0 in Fig. 4(c), but becomes flatter with the oxidation. In the heavy oxidation limit at A2, the CNT is in the accumulation mode and the band bending is slightly upward $\phi_{0A2} > 0$ in Fig. 4(d). It is clearly seen that Φ_{Bh} decreases appreciably in oxidation when $\chi_m - \phi_s - \zeta \leq 0$, corresponding to line "ka". Otherwise, the CNT is consistently in the accumulation mode, resulting in very little change in ϕ_0 as is the case for line "kb". In the n-CNT scenario, accumulation occurs for $\phi_0 < 0$ and negative $\sigma_{NT}(\phi_0)$ decreases very rapidly with decreasing ϕ_0, while inversion occurs for $\phi_0 > 0$ and positive $\sigma_{NT}(\phi_0) = +(2\varepsilon_{NT}\phi_0 N_B)^{1/2}$ is a horizontal parabola. In vacuum, $\sigma_{ox} = 0$ and $\sigma_{NT}(\phi_0)$ is line "$\beta 0$" in Fig. 4(b). As the oxidation progresses, $\sigma_{NT}(\phi_0) + \sigma_{ox}$ shifts downward and forms lines "$\beta 1$" and "$\beta 2$", and the intersection moves again downward from B0 through B1 to B2. The band structures at B0 with $\phi_{0B0} < 0$ and B1 with $\phi_{0B1} < 0$ are shown in Figs. 4(e) and 4(f), respectively. Unlike the p-CNT case, we should expect a significant change in ϕ_0 and therefore a significant Φ_{Be} modulation for various values of $\chi_m - \phi_s - \zeta$, for "ka" and "kb".

We will give analytical solutions by defining two positive energies, $U_B = e^2 N_B a^2 / 2\varepsilon_{tr}$ and $U_{OX} = ea\sigma_{ox}/\varepsilon_{tr}$. In the p-CNT scenario, accumulation ($\phi_0 > 0$) occurs for $-\chi_m + \phi_s + \zeta \geq U_{OX}$ and we can approximate $\phi_0 \sim 0$. Inversion ($\phi_0 < 0$) occurs for $-\chi_m + \phi_s + \zeta \leq U_{OX}$ and $(-\phi_0)^{1/2}$ satisfies a quadratic equation $(-\phi_0) + 2(U_B|\phi_0|)^{1/2} + \chi_m - \phi_s - \zeta + U_{OX} = 0$. Its solution is $(-\phi_0)^{1/2} = -U_B^{1/2} + (U_B - \chi_m + \phi_s + \zeta - U_{OX})^{1/2}$. In the n-CNT scenario, accumulation ($\phi_0 < 0$) occurs for $-\chi_m + \phi_s +$

$\zeta \geq U_{OX}$ and we can approximate $\phi_0 \sim 0$. Inversion ($\phi_0 > 0$) occurs for $- \chi_m + \phi_s + \zeta \leq U_{OX}$, and $\phi_0^{1/2}$ satisfies an equation $\phi_0 + 2(U_B\phi_0)^{1/2} - \chi_m + \phi_s + \zeta - U_{OX} = 0$. Its solution is $\phi_0^{1/2} = - U_B^{1/2} + (U_B + \chi_m - \phi_s - \zeta + U_{OX})^{1/2}$. In both scenarios, once ϕ_0 is obtained, $\Delta U = e\sigma_m(\phi_0)/C_G$ is determined and then Φ_{Bh} and Φ_{Be} are determined accordingly.

We will estimate the relevant numerical values. If Γ % of the CNT is covered with oxygen molecules $O_2^{\delta-}$, then $\sigma_{ox}/e = -1.86 \times 10^{13} \Gamma$ cm^{-2}. Then, the contribution of σ_{ox} upon ΔU is estimated to be 0.336 $a\Gamma\delta/\varepsilon_{tr}$ eV. With $a \sim$ 2-3 Å, $\Gamma \sim$ 10 %, $\delta \sim$ 0.01-0.1, and $\varepsilon_{tr} \sim$ 10, the contribution is a few tenths of an electron volt. Considering $E_G \sim$ 0.5 eV for a familiar (17,0) CNT [9], the present model successfully describes the reported effect of oxidation upon Φ_B [2].

So far, we have assumed that the oxygen molecules are physisorbed, but it is instructive to examine the chemisorbed case [10]. In this case, σ_{ox} is no longer a constant, but depends on ϕ_0 and ζ such that $\sigma_{ox}(\phi_0) = -en(\varepsilon_0 - \phi_0 - \zeta)/\varepsilon_0$, where $nd\varepsilon/\varepsilon_0$ is the number of energy levels per unit area with energies in the range $d\varepsilon$. Since $\sigma_{ox}(\phi_0)$ is a straight line with a gradient $-en/\varepsilon_0$, $\sigma_{NT} + \sigma_{ox}$ is steeper and ϕ_0 tends to be smaller in magnitude for a larger en/ε_0. Thus, ϕ_0 cannot be very different in air and in vacuum, and Φ_B is eventually pinned [11]. This is contrary to the experimental results [2], and it is expected that the oxygen molecules are either physisorbed or chemisorbed weakly with a low n in the typical experimental situations.

We have proposed a model for the Φ_B modulation in oxidation in the electrode – CNT system. The model considers a transition region at the Schottky junction and an appreciable potential can drop there. Oxidation increases this potential drop and therefore modifies Φ_B. We have explained the mechanism of low Φ_{Bh} in air and high Φ_{Bh} in vacuum successfully.

References

[a]CSC, Electronic address: yamada@nas.nasa.gov

[1] S. J. Tans, A. R. M. Verschueren, and C. Dekker, Nature (London) **393**, 49 (1998); R. Martel, T. Schmidt, H. R. Shea, T. Hertel, and Ph. Avouris, Appl. Phys. Lett. **73**, 2447 (1998); C. Zhou, J. Kong, and H. Dai, Appl. Phys. Lett. **76**, 1597 (2000); A. Bachtold, P. Hadley, T. Nakanishi, and C. Dekker, Science **294**, 1317 (2001).

[2] V. Derycke, R. Martel, J. Appenzeller, and Ph. Avouris, Nano Lett. **1**, 453 (2001); R. Martel, V. Derycke. J. Appenzeller, K. K. Chan, J. Tersoff, and Ph. Avouris, Phys. Rev. Lett. **87**, 256805 (2001); V. Derycke, R. Martel, J. Appenzeller, and Ph. Avouris, Appl. Phys. Lett. **80**, 2773 (2002); S. Heinze, J. Tersoff, R. Martel, V. Derkcke, J. Appenzeller, and Ph. Avouris, Phys. Rev. Lett. **89**, 106801 (2002).

[3] V_G induces charge $-C_{NT}V_G$ in the channel, where C_{NT} is a CNT capacitance, and this modifies the Fermi level. Thus, $\alpha \sim C_{NT}/[C_{NT} + e^2 D_0]$, where D_0 is a CNT state density at $V_G = 0$.

[4] G. Attard and C. Barnes, Surfaces, Oxford Chemistry Primes (Oxford, New York, 1998).

[5] S. M. Sze, *Physics of Semiconductor Devices*, 2nd ed. (Wiley, New York, 1981).

[6] W. H. Brattain and J. Bardeen, Bell Syst. Tech. J. **32**, 1 (1952).

[7] J. Bardeen, Phys. Rev. **71**, 717, (1947).

[8] A. Ricca, preprint. See also, A. Ricca and J. A. Dorocco, Chem. Phys. Lett. **367**, 217 (2002).

[9] M. S. Dresselhaus, G. Dresselhaus, and P. C. Eklund, *Science of Fullerenes and Carbon Nanotubes* (Academic, San Diego, 1996).

[10] S-H. Jhi, S. G. Louie, and M. L. Cohen, Phys. Rev. Lett. **85**, 1710 (2000).

[11] The Fermi level pinning due to the large surface states in the device geometry of Fig. 3 is possible as discussed in F. Leonard and J. Tersoff, Phys. Rev. Lett. **84**, 4693 (2000).
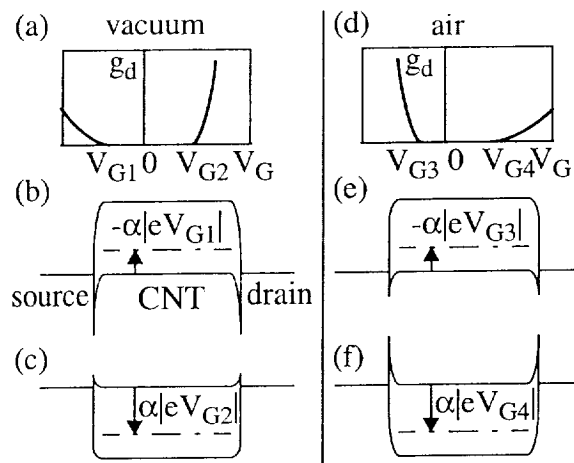
Figure Captions

FIG. 1. CNT FET characteristics in vacuum: (a) schematic channel conductance g_d as a function of gate voltage V_G in Ref. 2; (b) equilibrium band structure with the CNT conduction and valence edges at V_{G1}; (c) band structure at V_{G2}. CNT FET characteristics in air: (d) schematic $g_d(V_G)$ in Ref. 2; (e) band structures at V_{G3}; (f) band structure at V_{G4}.
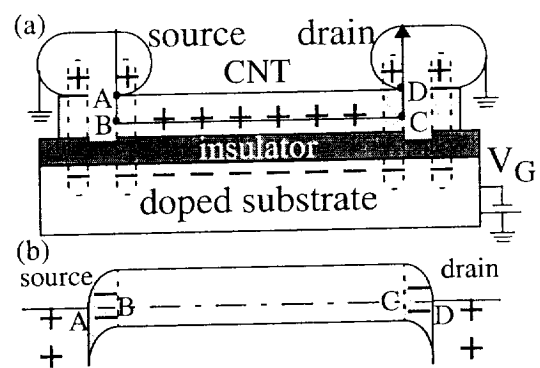
FIG. 2. Band structures for metallic electrode – semiconducting CNT Schottky junction based on the conventional view: (a) in vacuum and (b) in air. Proposed band structures showing a potential drop ΔU in the transition region: (c) in vacuum and (d) in air. a is the width, ε_{tr} is the dielectric constant, ϕ_s is the electron affinity, ζ is the Fermi level, χ_m is the work function, Φ_{Bh} is the hole Schottky barrier, and $O_2^{\delta-}$ indicates negatively charged oxygen molecules.

FIG. 3. CNT FET with gate voltage V_G in equilibrium: (a) real space charge distribution and (b) equivalent band structure along the arrow path above.
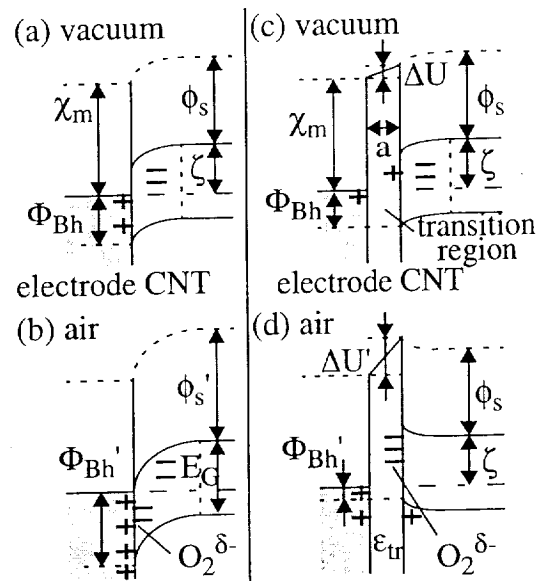
FIG. 4. Schematic plots of charge σ as a function of band bending ϕ_0: (a) p-CNT case and (b) n-CNT case. "αi" and "βi" (i = 0, 1, or 2) are CNT charge lines, and "ka" and "kb" are electrode charge lines. Band structures are shown for operating points: (c) A0 for p-CNT in vacuum; (d) A2 for p-CNT in air; (e) B0 for n-CNT in vacuum; (f) B1 for n-CNT in air. ϕ_s is the electron affinity, ζ is the Fermi level, χ_m is the work function, Φ_{Bh} is the hole Schottky barrier, Φ_{Be} is the electron Schottky barrier, and σ_{ox} is the negative charge on $O_2^{\delta-}$.
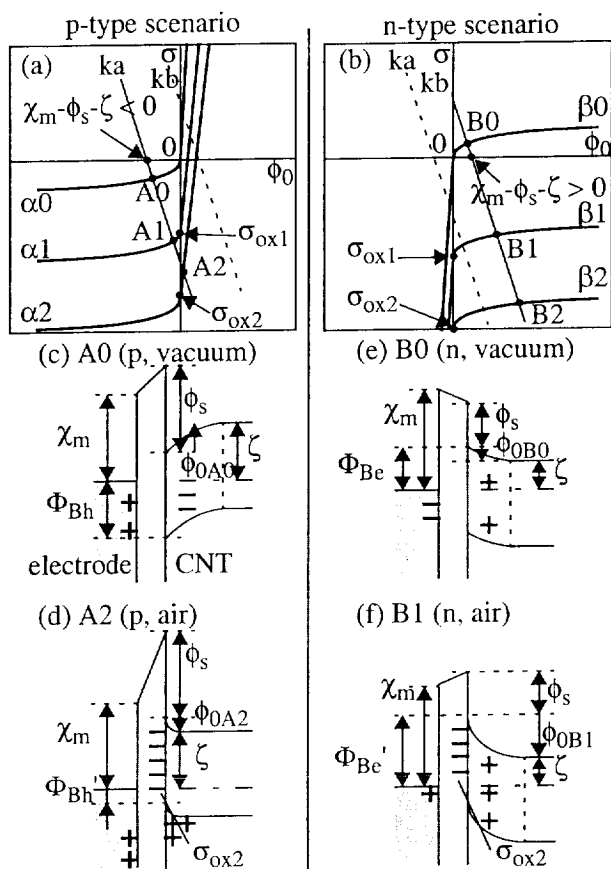
(a) vacuum

g_d

V_{G1} 0 V_{G2} V_G

(b)

$-\alpha|eV_{G1}|$

source | CNT | drain

(c)

$\alpha|eV_{G2}|$

(d) air

g_d

V_{G3} 0 V_{G4} V_G

(e)

$-\alpha|eV_{G3}|$

(f)

$\alpha|eV_{G4}|$

APL Yamada
Fig. 1

(a) source   drain
CNT
A
B
+ + + + + + +
insulator
doped substrate V_G

(b)
source   drain
A B — · — · — · — · — · C D +
+   +

(a) vacuum

(c) vacuum

(b) air

(d) air

APL Yamada
Fig. 2

APL Yamada
Fig. 4